SOUND SYNTHESIS FOR NONLINEAR PLATES

Stefan Bilbao

Sonic Arts Research Centre
Queen's University Belfast
United Kingdom

ABSTRACT

In this paper, a simple finite difference scheme for a rectangular dynamic nonlinear plate, under free boundary conditions is presented. The algorithm is straightforward to program, and is capable of reproducing, to a first approximation, the behaviour of various percussion instruments whose timbre depends crucially on nonlinear effects (due to high-speed strikes), including transient pitch glides and the buildup of high-frequency energy. Though computationally intensive, algorithms such as that presented here promise more faithful sound synthesis and, as with all physical model inspired synthesis algorithms, require the specification of only a few, physically meaningful parameters. Full details of the algorithm, including the setting of boundary conditions and computational demands are provided. Numerical simulation results are presented.

1. INTRODUCTION

In recent years, it has become possible to perform direct numerical simulations of increasingly complex mechanical systems in order to generate synthetic sound. For distributed nonlinear systems, traditional approaches such as modal synthesis [1] or digital waveguides [2] are difficult to apply (with some exceptions), and a direct approach would appear to be the only reliable way of capturing the complex dynamics of such systems.

Several percussion instruments, such as gongs, tam-tams and cymbals create sounds whose timbres are inextricably linked to nonlinear elastic vibration effects [3]. Though, strictly speaking, all these instruments are correctly modelled as shells [4] (i.e., plates with some curvature), a flat rectangular plate model is a fairly good starting point in the first instance, and can serve as the basis for more detailed instrument simulations. Such a model, as will be shown, is straightforward to program, and yields many effects which are characteristic of strongly nonlinear systems, including pitch glides, as well as an initial rapid buildup of high-frequency components.

In Section 2, the basic dynamic equation of a thin nonlinear plate is presented, and in Section 3, a difference scheme is developed. Particular attention is paid to the problem of setting boundary conditions, as this can be problematic under free edge conditions, and a simple necessary stability condition is presented, as well as a discussion of computational costs. Numerical simulation results are presented in Section 4.

2. NONLINEAR PLATE MODELS

A model for nonlinear plate dynamics, suitable for vibration of moderate amplitude of a thin plate (such as those which occur in musical instruments such as gongs), is the so-called dynamic analogue of the system of von Karman [5, 6]:

$$\ddot{w} = -\kappa^2\nabla^2\nabla^2 w + c^2\nabla^2 w - 2\sigma\dot{w} + b_1\nabla^2\dot{w} + \frac{1}{\rho}L[F,w] \quad (1)$$

Here $w(x,y,t)$ is the transverse plate deflection, defined over the rectangular region $x \in [0, L_x]$, $y \in [0, L_y]$ and for time $t \geq 0$. ∇^2 is the Laplacian, and $\nabla^2\nabla^2$ the biharmonic operator. The stiffness parameter κ^2 is defined by

$$\kappa^2 = \frac{Eh^2}{12\rho(1-\nu^2)}$$

where E, h, ρ and ν are Young's modulus, plate thickness, density and Poisson's ratio, respectively for the plate (assumed constant here). There are three extra linear terms which, though they are not often encountered in the literature, are of special interest in musical applications: the term involving the parameter c, with dimensions of velocity, represents a contribution to the dynamics due to constant applied tension, the term of coefficient σ controls the gross decay rate of plate oscillation, and that with coefficient b_1 allows for higher rates of loss at high frequencies (i.e., frequency-dependent damping). The function F is related to w, the plate deflection, by the so-called compatibility equation,

$$\nabla^2\nabla^2 F = -\frac{E}{2}L[w,w] \quad (2)$$

where the action of the operator $L[\cdot,\cdot]$ which appears in both (1) and (2) is defined by

$$L[\alpha,\beta] = \frac{\partial^2\alpha}{\partial x^2}\frac{\partial^2\beta}{\partial y^2} + \frac{\partial^2\alpha}{\partial y^2}\frac{\partial^2\beta}{\partial x^2} - 2\frac{\partial^2\alpha}{\partial x\partial y}\frac{\partial^2\beta}{\partial x\partial y} \quad (3)$$

Without the term in F, equation (1) is the equation of motion of a linear plate of Kirchhoff type, accompanied by the various axtra terms mentioned above, and can be thought of the 2D generalization of the equation for a stiff string or bar, such as that presented by Bensa et al. [7], and related to that of Chaigne and Askenfelt [8] and Ruiz [9]. The system of von Karman in polar coordinates has been used for the analysis of cymbal vibrations by Touze et al. [10], and it is worth noting that it is itself a simplified version of a more complex system for which in-plane

displacements are not neglected [11, 12]. There also exists an even more simplified form due to Berger [13, 6], for which the nonlinearity is modelled as an integral over the state of the plate, and which can be thought of as an extension to 2D of string or bar models of the Kirchhoff-Carrier type[14, 15]—such a model is undeniably much simpler to analyze and program, but it does not capture perceptually significant effects (though the important pitch-gliding effect is indeed well-reproduced).

We also note that we will discuss only the initial value problem in this paper (i.e., we model struck or "plucked" plates, and not those driven by an external forcing function, though it is straightforward to do so by adding an extra term of the form $f(x,t)$ on the right-hand side of (1)).

2.1. Initial and Boundary Conditions

The second order time-dependent PDE (1) requires two initial conditions, i.e.,

$$u(x,y,0) = u_0(x,y) \qquad \frac{\partial u}{\partial t}(x,y,0) = v_0(x,y)$$

It also requires the specification of two conditions for w at any boundary; in this paper, we consider boundary conditions of the free type [4](as are most common in musical instruments based on plate vibration, such as gongs):

$$\frac{\partial^2 w}{\partial x_n^2} + \nu \frac{\partial^2 w}{\partial x_s^2} = 0 \tag{4a}$$

$$\frac{\partial^3 w}{\partial x_n^3} + (2-\nu)\frac{\partial^3 w}{\partial x_s^2 \partial x_n} = 0 \tag{4b}$$

where $\frac{\partial^2}{\partial x_n^2}$ and $\frac{\partial^2}{\partial x_s^2}$ represents second spatial partial derivatives in directions normal to and tangential to a given boundary (in this case, rectangular).

Two boundary conditions for F must also be supplied; these can be written as

$$\frac{\partial^2 F}{\partial x_s^2} = \frac{\partial^2 F}{\partial x_s \partial x_n} = 0 \tag{5}$$

It has been noted by Thomas et al. [16] that these conditions can be reduced to simpler conditions of the form

$$F = \frac{\partial F}{\partial x_n} = 0 \tag{6}$$

due, apparently, to the fact that F is a potential function. Note that only the second spatial derivatives of F appear in (1), so the dynamics are undisturbed under the addition of any bilinear function in x and y to F—such a bilinear function may be used to obtain the simplified conditions found above.

In the case of the rectangular plate under free boundary conditions, it is also possible to show [5] that due to the absence of so-called "corner forces," it must also be true that at any corner,

$$\frac{\partial^2 w}{\partial x \partial y} = 0 \tag{7}$$

This condition is of special importance with regard to a finite difference approximation which takes a grid point at the corner (see Section 3.4).

3. FINITE DIFFERENCE SCHEMES

Finite difference schemes for plate equations have a long history, and are well summarized in the linear case by Szilard [5]. Though in the industrial world, they have long since been superseded by finite element methods, which are ideal for modelling materials of complex geometry, it is true that many percussion instruments are of a relatively simple geometry, and can thus be dealt with rather elegantly in regular coordinate systems using straightforward difference methods. Though a simple finite difference scheme is presented here, it should be kept in mind that there are other methods which are well-suited to simple geometric configurations, most notably pseudospectral methods [17, 18]; such methods were applied to the dynamic von Karman equations by Kirby et al. [12].

3.1. Grid Functions and Difference Operators

In order to solve (1) numerically, we can make use of a finite difference approximation, first defining a grid function $u_{i,j}^n$ representing an approximation to a continuously variable function $u(x,y,t)$ at coordinates $x = i\Delta$, $y = j\Delta$, and $t = nT$ (u, in this case, stands for either of F or w, the two variables which must be approximated in Equations (1) and (2)). Here, Δ is the grid spacing in the x and y directions, respectively, and T is the time step ($1/T$ is the sample rate). (It is possible to set different values of Δ in the two coordinate directions, but for simplicity, it is assumed that they are equal.)

Standard approximations to the first and second time differential operators are given by

$$\begin{aligned}
\delta_t^2 u_{i,j}^n &= \frac{1}{T^2}\left(u_{i,j}^{n+1} - 2u_{i,j}^n + u_{i,j}^{n-1}\right) \approx \frac{\partial^2 u}{\partial t^2} \\
\delta_{t0} u_{i,j}^n &= \frac{1}{2T}\left(u_{i,j}^{n+1} - u_{i,j}^{n-1}\right) \approx \frac{\partial u}{\partial t} \\
\delta_{t-} u_{i,j}^n &= \frac{1}{T}\left(u_{i,j}^{n} - u_{i,j}^{n-1}\right) \approx \frac{\partial u}{\partial t}
\end{aligned}$$

The first and second operators above are centered and second-order accurate; the third, a backward difference operator, is first-order accurate. Second-order centered difference approximations to first and second derivatives in the x and y directions are given by

$$\begin{aligned}
\delta_{x0} u_{i,j}^n &= \frac{1}{2\Delta}\left(u_{i+1,j}^n - u_{i-1,j}^n\right) \approx \frac{\partial u}{\partial x} \\
\delta_{y0} u_{i,j}^n &= \frac{1}{2\Delta}\left(u_{i,j+1}^n - u_{i,j-1}^n\right) \approx \frac{\partial u}{\partial y} \\
\delta_x^2 u_{i,j}^n &= \frac{1}{\Delta^2}\left(u_{i+1,j}^n - 2u_{i,j}^n + u_{i-1,j}^n\right) \approx \frac{\partial^2 u}{\partial x^2} \\
\delta_y^2 u_{i,j}^n &= \frac{1}{\Delta^2}\left(u_{i,j+1}^n - 2u_{i,j}^n + u_{i,j-1}^n\right) \approx \frac{\partial^2 u}{\partial y^2}
\end{aligned}$$

The mixed derivative, Laplacian and biharmonic operators can be approximated by

$$\begin{aligned}
\delta_{x0}\delta_{y0} &\approx \frac{\partial^2}{\partial x \partial y} \\
\delta_+^2 = \delta_x^2 + \delta_y^2 &\approx \nabla^2 \\
\delta_+^2 \delta_+^2 &\approx \nabla^2 \nabla^2
\end{aligned} \tag{8}$$

3.2. A Nonlinear Finite Difference Scheme

At this point, we may substitute the above operators for their continuous time/space counterparts in (1) and (2), to get the following explicit finite difference scheme:

$$\delta_t^2 w = -\kappa^2 \delta_+^2 \delta_+^2 w + c^2 \delta_+^2 w - 2\sigma \delta_{t0} w + b_1 \delta_{t-} \delta_+^2 w + \frac{1}{\rho} L[F, w] \tag{9}$$

with

$$\delta_+^2 \delta_+^2 F = -\frac{E}{2} L[w, w] \tag{10}$$

Now, the operator $L[\cdot, \cdot]$ is defined in terms of its operation on two grid functions α and β by

$$L[\alpha, \beta] = (\delta_x^2 \alpha)(\delta_y^2 \beta) + (\delta_y^2 \alpha)(\delta_x^2 \beta) - 2(\delta_{x0} \delta_{y0} \alpha)(\delta_{x0} \delta_{y0} \beta)$$

Difference equation (9) can be rewritten as an explicit recursion in the grid function $w_{i,j}^n$, where an interior point in the domain (we will define this presently) is updated according to

$$\begin{aligned} w_{i,j}^{n+1} &= \eta \sum_{|k|+|l| \le 2} \beta_{|k|,|l|} w_{i+k,j+l}^n \\ &\quad + \eta \sum_{|k|+|l| \le 1} \gamma_{|k|,|l|} w_{i+k,j+l}^{n-1} + \frac{T^2}{\rho} L[F, w]^n \end{aligned} \tag{11}$$

where

$$\begin{aligned} \beta_{0,0} &= 2 - 20\mu^2 - 4(\lambda^2 + \epsilon) \\ \beta_{1,0} &= \beta_{0,1} = 8\mu^2 + \lambda^2 + \epsilon \\ \beta_{1,1} &= -2\mu^2 \\ \beta_{2,0} &= \beta_{0,2} = -\mu^2 \\ \gamma_{0,0} &= -1 + 4\epsilon + \sigma T \\ \gamma_{1,0} &= \gamma_{0,1} = -\epsilon \end{aligned}$$

and where we have also defined

$$\begin{aligned} \mu &= \frac{\kappa T}{\Delta^2} \qquad & \lambda &= \frac{cT}{\Delta} \\ \eta &= \frac{1}{1 + \sigma T} \qquad & \epsilon &= \frac{b_1 T}{\Delta^2} \end{aligned}$$

The updating of scheme (11) also requires access to $F_{i,j}^n$. But $F_{i,j}^n$ may be computed from previously calculated values of $w_{i,j}^n$ through (10); this, however, requires the inversion of the operator $\delta_+ \delta_+$, subject to boundary conditions on F (this will be discussed further in Section 3.4). As such, the inversion of the biharmonic constitutes the most computationally costly step in the algorithm, which is otherwise completely explicit.

Difference scheme (9) accompanied by (10) is formally second order accurate in space and first-order accurate in time, due to the use of the operator δ_{t-}, necessary in order to obtain an explicit algorithm. Since the term involving δ_{t-} is in general a small perturbation, we do not expect such a term to have a deleterious effect on accuracy as a whole.

3.3. Stability

A full stability analysis of the above finite difference scheme is complicated by the nonlinearity (though it may be possible to use energetic principles in order to derive a similar scheme with global stability, as has been done in the case of the nonlinear string [19]). As such, it it is important to at least ensure stability for the linear problem (i.e., (9) in the absence of the final nonlinear term). Through simple von Neumann analysis [20, 21], it is possible to show that such a condition can be phrased in terms of the time step T and the grid spacing Δ by

$$\Delta^2 \ge 2b_1 T + c^2 T^2 + \sqrt{(2b_1 T + c^2 T^2)^2 + 16\kappa^2 T^2} \tag{12}$$

In practice, for audio simulation, the time step T is fixed by the sample rate, and thus Δ must be chosen so as not to violate (12).

It is important to note that the finite difference scheme (9) does become unstable under very large amplitude vibration (i.e., when the amplitude of the vibration becomes greater than the plate thickness). In effect, this instability reflects the limited validity of the von Karman model itself, which is intended to deal with moderately large amplitude vibration (which is indeed the case for most musical instruments).

3.4. Boundary Conditions

Scheme (9) holds at interior points in the domain, i.e., those which are located at least two grid points away from a boundary. Updating scheme (9) at points near the boundary requires access to so-called "image" points beyond the boundary at the previous time step—the values at these points may be set in the standard way, using approximations to (4) at grid points along the edge:

$$\delta_n^2 w + \nu \delta_s^2 w = 0 \tag{13a}$$

$$\delta_{n0} \delta_n^2 w + (2 - \nu) \delta_{n0} \delta_s^2 w = 0 \tag{13b}$$

where again, n and s refer to coordinates normal to and tangential to the boundary. Taking, for instance, a center point on the western boundary of the plate, at location $i = 0$, j (see Figure 1), these may be rewritten as

$$w_{-1,j}^n = 2w_{0,j}^n - w_{1,j}^n - \nu(w_{0,j+1}^n - 2w_{0,j}^n + w_{0,j-1}^n) \tag{14a}$$

$$\begin{aligned} w_{-2,j}^n = {} & 2w_{-1,j}^n - 2w_{1,j}^n + w_{2,j}^n \\ & -(2 - \nu)(w_{-1,j+1}^n - 2w_{-1,j}^n + w_{-1,j-1}^n \\ & \qquad - w_{1,j+1}^n + 2w_{1,j}^n - w_{1,j-1}^n) \end{aligned} \tag{14b}$$

Referring to Figure 1, one may proceed as follows. First set the values of points labelled A, through an application of condition (14a). Then, in order to set the grid variables at points B, note that boundary condition (14a) centered at the corner implies that both $\delta_n^2 w$ and $\delta_s^2 w$ are zero at the boundary, so that these values may be set using only values of the grid function directly on the edge. In order set the value at the point with coordinates $i = -1$, $j = 0$, one may write, then,

$$w_{-1,0}^n = 2w_{0,0}^n - w_{1,0}^n \tag{15}$$

Once the values at points A and B have been set, the values at points C may be then set through an application of the

discrete boundary condition corresponding to (7), using the discrete mixed derivative defined by (8). At the point with coordinates $i = -1$, $j = -1$, one may then write

$$w^n_{-1,-1} = -w^n_{1,1} + w^n_{1,-1} + w^n_{-1,1} \tag{16}$$

Finally, one may then directly set the values at points D through a direct application of (14b), which refers to interior points as well as values set at points A, B and C.

It is worth noting that although it is not necessary to store grid variables at the image locations (normally, one simply reflects their set values back into the interior, thus modifying the behavior of any differential operator acing in the vicinity of the boundary), it may be useful to do so for debugging purposes, and also because explicit storage of such values allows for an efficient application of 2D convolution in order to avoid specialized boundary schemes).

Solving for $F^n_{i,j}$ is a matter of writing a matrix equation for (10), and solving the linear system in terms of the already computed vales of $w^n_{i,j}$. As $F^n_{i,j}$ is assumed to be zero on the boundaries, the problem is restricted to solving for $F^n_{i,j}$ strictly in the interior. As the discrete biharmonic difference operator requires access to points which are at most two steps away in either the x or y directions, in order to write its form subject to the boundary conditions, a single layer of image points adjacent to the edge will be necessary, and may be set in accord with the second condition of Equation 6, e.g., one may write $F^n_{1,j} = F^n_{-1,j}$ at points adjacent to the western boundary.

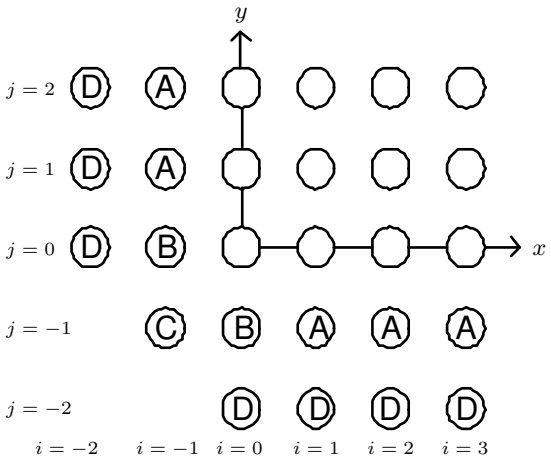

Figure 1: *Bottom left-hand corner of a computational grid. Unlabelled circles represent interior grid points, and those labelled A to D are image points required in order to update scheme* (9) *in the interior.*

It is important to mention that under free boundary conditions, the plate is able to undergo rigid body motion; though such motion is inaudible (if one takes the deflection of the plate at a given point as an audio output), it leads to significant "DC" drift, which can be problematic in fixed point arithmetic. A simple solution is to apply a DC-blocking filter to the output soundfile (or a high-pass filter), taking care not to remove any of the low-frequency audible energy generated as subharmonics (which constitute yet another interesting perceptual effect replicated under this model).

3.5. Computational Considerations

The computational requirements for such a simulation depend on the sample rate, plate dimensions, and material parameters (primarily the stiffness). For a plate of dimensions L_x, L_y, there will be approximately $L_x L_y/\Delta^2$ grid points to be updated each time step. If Δ has been chosen at its minimum value according to (12) (and assuming, for simplicity, that $c = b_1 = 0$), then the total number of points will be $L_x L_y/(4\kappa T)$. The linear part of the update (i.e., the difference scheme (11), without the nonlinear term), requires approximately six multiplies per point, per time step, giving a total operation count of $3L_x L_y/(2\kappa T^2)$ operations per second. Solving the nonlinear part, however, from (10), if implemented directly as a matrix multiply (the inverse of the biharmonic may be computed offline and stored) will require $L_x^2 L_y^2/(16\kappa^2 T^3)$ operations per second, and is clearly the dominant factor. For a 0.5 m $\times$ 0.5 m steel plate, of thickness 0.005 m, and at a sample rate of 44.1 kHz, approximately 6 billion operations per second will be required—this is out of real time for most desktop computers, but not by a large factor. Reducing the sample rate, as well as the plate size can have a dramatic effect on computational cost, as should be clear from the expression given above. Also, given that the biharmonic difference operator, as defined here, is extremely sparse, and has a good deal of structure (e.g., it is nearly of Toeplitz-block-Toeplitz form), faster methods for linear system solution, perhaps based on the matrix inversion lemma [22] and the FFT, should be applicable.

4. NUMERICAL RESULTS

The most musically important effect which distinguishes this nonlinear plate model from a linear one is the generation of high-frequency components given an initial excitation which does not possess them; such is the cause of the characteristic "shimmer" or gong sounds, for instance. As an illustration of this effect, we have run a simulation of a steel plate ($E = 2 \times 10^{11}$ N/m^2, $\rho = 7.86 \times 10^3$ kg/m^3, $\nu = 0.3$), of thickness $h = 0.005$ m, and of dimensions $L_x = L_y = 0.4$ m. In order to best illustrate the buildup of high-frequency components, the plate has been excited by an initial velocity distribution in the form of $v_0 \sin(\pi x/L_x)^2 \sin(\pi y/L_y)^2$, which, although it only approximately satisfies the boundary conditions, is of simple form and gives rise to primarily low-order components (at least in the linear case). The sample rate is 44.1 kHz. In Figure 2 are shown spectrograms of 1.0 s of the resulting synthesis output (read from the plate center), under linear conditions (top panel), under a moderate velocity of $v_0 = 20$ m/s and a high velocity of $v_0 = 70$ m/s. Notice in particular, the frequency-dependent decay (due to the term of coefficient b_1 in (1)), and in the final plot, the rapid buildup of harmonics in the initial 50 ms.

The characteristic buildup time of the upper partials is perceptually relevant, and is captured by this simple nonlinear plate model; in general, the larger the plate, the longer

the buildup time. In Figure 3 are shown spectrograms of the first 300 ms of synthetic sounds, generated under the same conditions as the previous example, except for plate size (0.5 m × 0.5 m in the left-hand panel, and 1.5 m × 1.5 m in the right-hand panel), and sample rate (18 kHz).

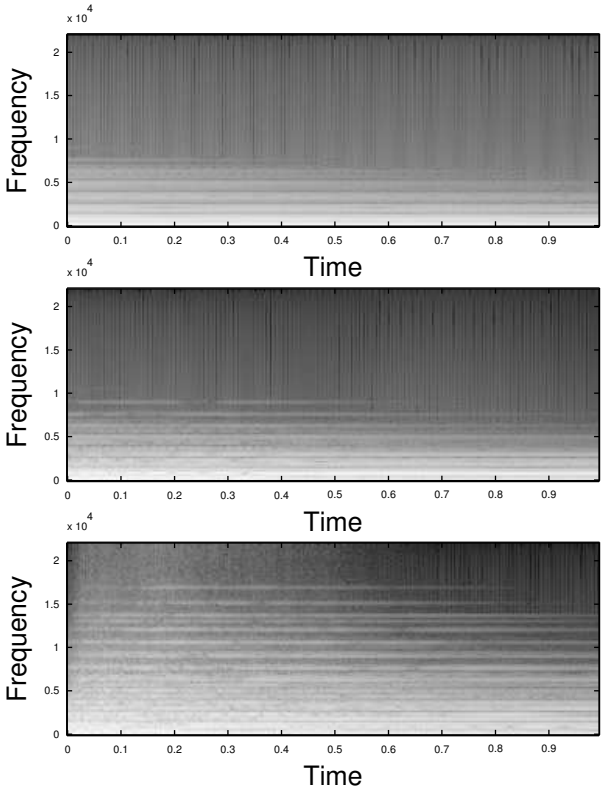

Figure 2: *Spectrograms for synthetic struck plate sounds, under linear conditions (top), low velocity striking (middle) and high velocity striking (bottom).*

Another interesting phenomenon, that of downwards pitch glide, is exhibited in the spectrogram shown in Figure 4. In this case, the plate is again made of steel, and is of the same thickness is the same as in the previous examples, but of dimensions 0.15 m × 0.15 m (chosen small so that individual partials may be easily seen in spectral plots), and is struck with an initial velocity distribution in the form of a raised 2D cosine, of radius one-quarter of the plate side length (in order provide initial energy immediately to the upper partials). The sample rate is chosen as 44.1 kHz. Under extreme initial velocity conditions (here, 350 m/s), a noticeable pitch descent of perhaps a full tone is observed in the upper partials over the first half second. It is difficult to determine the nature of the initial wavering of the upper partials, but a good guess would be that these indicate the onset of numerical stability (indeed, for velocities higher than 350 m/s, the algorithm becomes unstable).

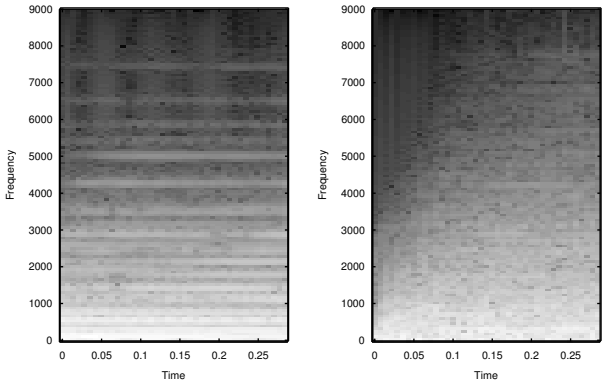

Figure 3: *Spectrograms for initial segments of synthetic struck plate sounds, for small plate (left) and a large one (right).*

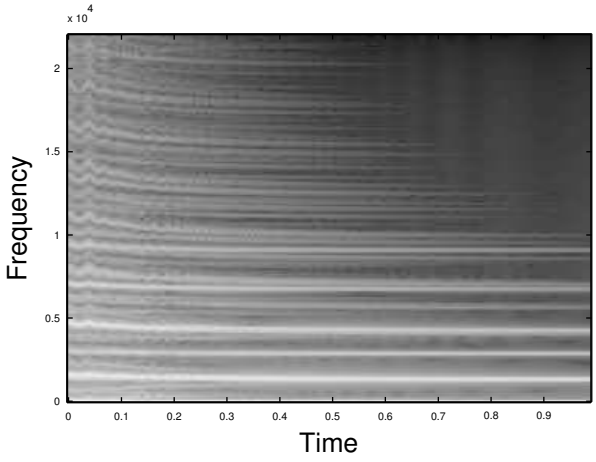

Figure 4: *Spectrogram for a synthetic struck plate sound, showing initial wavering of partial frequencies, as well as downward glides.*

5. CONCLUSIONS AND FUTURE DIRECTIONS

In this paper, a simple finite difference scheme for sound synthesis based on nonlinear plate vibration has been described, and simulation results have been presented. Though computationally intensive, the sounds generated are extremely rich, and the algorithm is able to replicate many subtle effects, including initial pitch glides and upper harmonic generation, which are not captured by simpler linear models.

The main problems, in the opinion of this author, are computational expense, and numerical stability issues. The first of these concerns is of a fundamental nature, and is difficult to avoid—though there are certainly opportunities for efficiency gains (by, say, fast linear system inversion techniques mentioned in Section 3.5), any true simulation of a complex physical system of this nature will be costly. It is

perhaps better, then, to simply accept this cost, and wait for future improvement in computational speeds. Numerical stability, for nonlinear systems such as the von Karman plate, is a more delicate matter. Though, upon familiarizing oneself with the algorithm presented here, one can develop some intuition for conditions under which the algorithm becomes unstable (relating mainly to the size of the initial conditions), there is no general stability condition that can be applied. To this end, a future direction of this author will be towards the development of difference schemes for plates via the energy method [23, 24], for which convenient stability conditions may be expressed purely in terms of the Courant number—this has been accomplished in the case of nonlinear strings [19]. This would appear to be an important step that must be taken before an algorithm such as this can be of use to a musician.

There are, of course, many different directions in which the algorithm presented here can be generalized: to plates of variable thickness (as is the case for gong-like instruments with a raised central dome), to plates of circular geometry, and, most importantly, to nonlinear shells, in order to capture the effects of curved gong rims, as well as cymbals. Further important steps, namely the development of parameterized software modules and also specialized hardware are also currently being undertaken.

6. ACKNOWLEDGEMENTS

Special thanks to Professor Carlos Felippa, at the University of Colorado at Boulder, and Professor Antoine Chaigne, at ENSTA.

7. REFERENCES

[1] J.-M. Adrien, "The missing link: Modal synthesis," in *Representations of Musical Signals*, G. DePoli, A. Picialli, and C. Roads, Eds., pp. 269–297. MIT Press, Cambridge, MA, 1991.

[2] J. O. Smith III, *Physical Audio Signal Procesing*, draft version, Stanford, CA, 2004, Available online at http://ccrma.stanford.edu/~jos/pasp04/.

[3] T. Rossing, F. Moore, and P. Wheeler, *The Science of Sound*, Addison-Wesley, San Francisco, California, third edition.

[4] K. Graff, *Wave Motion in Elastic Solids*, Dover, New York, New York, USA, 1975.

[5] R. Szilard, *Theory and Analysis of Plates*, Prentice Hall, Englewood Cliffs, New Jersey, 1974.

[6] A. Nayfeh and D. Mook, *Nonlinear Oscillations*, John Wiley and Sons, New York, New York, 1979.

[7] J. Bensa, S. Bilbao, R. Kronland-Martinet, and J. O. Smith III, "The simulation of piano string vibration: From physical models to finite difference schemes and digital waveguides," *Journal of the Acoustical Society of America*, vol. 114, no. 2, pp. 1095–1107, 2003.

[8] A. Chaigne and A. Askenfelt, "Numerical simulations of struck strings. I. A physical model for a struck string using finite difference methods," *Journal of the Acoustical Society of America*, vol. 95, no. 2, pp. 1112–8, Feb. 1994.

[9] P. Ruiz, "A technique for simulating the vibrations of strings with a digital computer," M.S. thesis, University of Illinois, 1969.

[10] C. Touze, O. Thomas, and A. Chaigne, "Asymmetric nonlinear forced vibrations of free-edge circular plates. part i. theory," *Journal of Sound and Vibration*, vol. 258, no. 4, pp. 649–676, 2002.

[11] Y. Zhiming, "A nonlinear dynamical theory of nonclassical plates," *Journal of Shangai University*, vol. 1, no. 2, pp. 1–17, 1997.

[12] R. Kirby and Z. Yosibash, "Solution of von-karman dynamic non-linear plate equations using a pseudospectral method," *Computer Methods in Applied Mechanics and Engineering*, vol. 193, no. 6–8, pp. 575–599, 2004.

[13] H. Berger, "A new approach to the analysis of large deflections of plates," *Journal of Applied Mathematics*, vol. 22, pp. 465–472, 1955.

[14] G. Kirchhoff, *Vorlesungen über Mechanik*, Tauber, Leipzig, 1883.

[15] G. F. Carrier, "On the nonlinear vibration problem of the elastic string," *Quarterly of Applied Mathematics*, vol. 3, pp. 157–165, 1945.

[16] O. Thomas, C. Touze, and A. Chaigne, "Asymmetric nonlinear forced vibrations of free-edge circular plates. part i. experiments," *Journal of Sound and Vibration*, vol. 265, pp. 1075–1101, 2003.

[17] L. Trefethen, *Spectral Methods in Matlab*, SIAM, Philadelphia, Pennsylvania, USA, 2000.

[18] B. Fornberg, *A Practical Guide to Pseudospectral Methods*, Cambridge Monographs on Applied and Computational Mathematics, Cambridge, England, 1995.

[19] S. Bilbao and J. O. Smith III, "Energy-conserving finite difference schemes for nonlinear strings," *Acustica*, 2004, Accepted for publication, revised.

[20] R. Vichnevetsky and J. Bowles, *Fourier Analysis of Numerical Approximations of Hyperbolic Equations*, SIAM, Philadelphia, 1982.

[21] J. Strikwerda, *Finite Difference Schemes and Partial Differential Equations*, Wadsworth and Brooks/Cole Advanced Books and Software, Pacific Grove, Calif., 1989.

[22] R. Horn and C. Johnson, *Matrix Analysis*, Cambridge University Press, Cambridge, England, 1985.

[23] B. Gustaffson, H.-O. Kreiss, and J. Oliger, *Time Dependent Problems and Difference Methods*, John Wiley and Sons, New York, 1995.

[24] S. Li and L. Vu-Quoc, "Finite difference calculus invariant structure of a class of algorithms for the nonlinear Klein Gordon equation," *SIAM J. Num. Anal.*, vol. 32, pp. 1839–1875, 1995.